Cancer Research

AACR

A Comprehensive View of Nuclear Receptor Cancer Cistromes

Qianzi Tang, Yiwen Chen, Clifford Meyer, et al.

Updated Version	Access the most recent version of this article at: doi:10.1158/0008-5472.CAN-11-2091
Supplementary Material	Access the most recent supplemental material at: http://cancerres.aacrjournals.org/content/suppl/2011/09/22/0008-5472.CAN-11-2091.DC1.html

Cited Articles	This article cites 20 articles, 5 of which you can access for free at: http://cancerres.aacrjournals.org/content/71/22/6940.full.html#ref-list-1

E-mail alerts	Sign up to receive free email-alerts related to this article or journal.
Reprints and Subscriptions	To order reprints of this article or to subscribe to the journal, contact the AACR Publications Department at pubs@aacr.org.
Permissions	To request permission to re-use all or part of this article, contact the AACR Publications Department at permissions@aacr.org.

A Comprehensive View of Nuclear Receptor Cancer Cistromes

Qianzi Tang[1], Yiwen Chen[2], Clifford Meyer[2], Tim Geistlinger[3], Mathieu Lupien[3], Qian Wang[1], Tao Liu[2], Yong Zhang[1], Myles Brown[3], and Xiaole Shirley Liu[2]

Abstract

Nuclear receptors comprise a superfamily of ligand-activated transcription factors that play important roles in both physiology and diseases including cancer. The technologies of chromatin immunoprecipitation followed by array hybridization (ChIP-chip) or massively parallel sequencing (ChIP-seq) has been used to map, at an unprecedented rate, the *in vivo* genome-wide binding (cistrome) of nuclear receptors in both normal and cancer cells. We developed a curated database of 88 nuclear receptor cistrome data sets and other associated high-throughput data sets including 121 collaborating factor cistromes, 94 epigenomes, and 319 transcriptomes. Through integrative analysis of the curated nuclear receptor ChIP-chip/seq data sets, we discovered novel factor-specific noncanonical motifs that may have important regulatory roles. We also revealed a common feature of nuclear receptor pioneering factors to recognize relatively short and AT-rich motifs. Most nuclear receptors bind predominantly to introns and distal intergenetic regions, and binding sites closer to transcription start sites were found to be neither stronger nor more evolutionarily conserved. Interestingly, while most nuclear receptors appear to be predominantly transcriptional activators, our analysis suggests that the binding of ESR1, RARA, and RARG has both activating and repressive effects. Through meta-analysis of different omic data of the same cancer cell line model from multiple studies, we generated consensus cistrome and expression profiles. We further made probabilistic predictions of the nuclear receptor target genes by integrating cistrome and transcriptome data and validated the predictions using expression data from tumor samples. The final database, with comprehensive cistrome, epigenome, and transcriptome data sets and downstream analysis results, constitutes a valuable resource for the nuclear receptor and cancer community. *Cancer Res; 71(22); 6940–7. ©2011 AACR.*

Introduction

Nuclear receptors form a large class of transcription factors that can bind directly to DNA to regulate gene expression upon ligand activation. The ligands can be steroid, hormones, or other molecules, although some nuclear receptors, called orphan receptors, have no known ligands. The human and mouse genomes encode 48 and 49 nuclear receptors, respectively. These nuclear receptors play important roles in the development, homeostasis, and metabolism of higher organisms.

Nuclear receptors play key roles not only in normal physiology but also in many pathologic processes, most notably cancer. Estrogen receptor (ESR) is overexpressed in more than 70% of breast cancers and is the archetypal molecular therapeutic target (1). Progesterone receptor has been shown to enhance breast cancer motility and invasiveness (2). Androgen receptor overactivation by androgens is essential for the initiation and progression of prostate cancers (3, 4). Retinoic acid receptor (RAR), upon activation by retinoic acid (RA), has antiproliferative effects in tumor cells (5). The translocation and subsequent oncofusion of promyelocytic leukemia (PML) with RARα in hematopoietic myeloid cells causes acute promyelocytic leukemia (6). Recent studies have linked cancer to lipid metabolism and cell inflammations (7, 8), and the

Authors' Affiliations: [1]Department of Bioinformatics, School of Life Science and Technology, Tongji University, Shanghai, China; and Departments of [2]Biostatistics and Computational Biology and [3]Medical Oncology, Dana-Farber Cancer Institute, Harvard Medical School, Boston, Massachusetts

Corresponding Authors: Xiaole Shirley Liu, Department of Biostatistics and Computational Biology, Dana-Farber Cancer Institute, Harvard School of Public Health, 44 Binney St., Boston, MA 02115. Phone: 617-632-2472; Fax: 617-632-2444; E-mail: xsliu@jimmy.harvard.edu and Myles Brown, Department of Medical Oncology, Dana-Farber Cancer Institute, Harvard Medical School, 44 Binney St., Boston, MA 02115. Phone: 617-632-3948; Fax: 617-632-5417; E-mail: myles_brown@dfci.harvard.edu

American Association for **Cancer Research**

major nuclear receptors regulating these processes include glucocorticoid receptor (GR), PPAR, and liver X-receptor (LXR; ref. 9).

Nuclear receptors often bind to DNA as homo- or heterodimers, each recognizing a half-site of 6 nucleotides. Thus, their DNA-binding sequences, called hormone response elements, often consist of 2 half-sites in directed, everted, or inverted configurations, separated by a variable gap (10). Much effort has been devoted to *de novo* prediction of nuclear receptor–binding sites, based solely on genomic DNA sequence, without much success. Recently, the application of ChIP-chip/seq techniques has enabled the accurate and effective detection of the genome-wide *in vivo* binding sites or cistromes of nuclear receptors (Supplementary Table S1). Herein, we define the cistrome as the set of *cis*-acting elements bound by a *trans*-factor at the genomic scale, that is, binding sites identified by ChIP-chip/seq experiments. Publicly available cistrome data have been growing rapidly, and sometimes multiple cistrome profiles of the same *trans*-factor in the same biological system are available. Meta-analysis of related cistrome profiles can often yield much more biologically relevant insights than the examination of single profiles.

Previous efforts to identify nuclear receptor target genes have mostly relied on differential expression profiles before and after nuclear receptor activation. However, the differential expression cutoff value selected may not be ideal, and for many genes, differential expression may be due to secondary or tertiary effects of nuclear receptor activity. With the availability of cistrome data, target gene prediction based on the presence of a binding site within a certain distance from the transcription start site (TSS) of the gene has also been used, although the distance cutoff value is often arbitrary. In addition, many genes with nearby binding sites show no differential expression upon binding, due to the gene's promoter chromatin status, missing essential cofactors, and other confounding effects. Intuitively, the combination of cistrome and differential expression profiles should allow for a much more robust prediction of the direct target genes of nuclear receptors than either data alone.

In this study, we systematically collected and preprocessed all of the publicly available genome-wide ChIP-chip/seq data for nuclear receptors, their collaborating factors, and histone modifications in humans and mice using a standardized computational pipeline. We compared the hormone response element patterns, distance (to TSSs of genes) distributions, evolutionary conservation, and collaborating partners of different nuclear receptors. We also conducted meta-analyses to generate consensus cistrome and expression profiles. Finally, we integrated cistrome and transcriptome data to make probabilistic predictions of nuclear receptor target genes, including 10 nuclear receptors in various cancer cell line models. The resultant cistromes, epigenomes, transcriptomes, motif analyses, and target gene lists are publicly available at Nuclear Receptor Cancer Cistromes (11).

Materials and Methods

Target gene prediction

In some systems such as ESR1 activation in the breast cancer cell line MCF7, multiple cistrome and transcriptome data are available from different studies using the same or different platforms. We first used the Stouffer P value combination method (12) to combine different transcriptome data sets, giving each gene a consensus differential expression z-score. We also used MM-ChIP (13) to combine redundant cistrome data sets to create a consensus peak list. On the basis of the characterization of higher order chromatin interactions and our preliminary analysis, we calculated the regulatory potential for a given gene, S_g, as the sum of the nearby binding sites weighted by the distance from each site to the TSS of the gene: $S_g = \sum_{i=1}^{k} e^{-(0.5+4\Delta_i)}$, where k is the number of binding sites within 100 kb of gene g and Δ_i is the distance between site i and the TSS of gene g normalized to 100 kb (e.g., 0.5 for a 50-kb distance). This equation models the influence of each binding site on gene regulation as a function that decreases monotonically with increasing distance from the TSS. The shape of this function approximates empirical observations of the distance between binding sites and differentially expressed genes in multiple ChIP-seq experiments. The constant in the equation enables the exponential function to adopt more flexible shapes and 0.5 was derived to better fit ChIA-PET and Hi-C data. As rank product was finally used to predict targets, the exact value of this constant would not change the regulatory potential ranking of genes. Incorporating binding affinity into the model does not significantly improve the prediction power and therefore were excluded from the model. We represented each gene using the following 2 parameters: (i) the differential gene expression z-score (if multiple transcriptome data are available) or t-value (if single transcriptome data are available) and (ii) the regulatory potential. For target prediction, we only considered genes with at least one binding site within 100 kb from its TSS and a differential expression z-score or t-value above the 75th percentile. We applied the Breitling rank product method (14, 15) to combine transcription factor–binding potentials with differential expression values (shown in Fig. 3A is an example of the rank product result from integration of one ESR ChIP-chip data set and one differential expression data set of estrogen 12-hour treatment). The false discovery rate of each predicted target is estimated by a permutation method proposed in the work of Breitling and colleagues (14).

Results

Data set summary

We collected a total of 88 cistrome data sets for 13 nuclear receptors, 121 cistrome data sets for 21 collaborating factors, and 94 genome-wide analyses of 12 histone modifications, which were profiled in the same cell systems as the nuclear

Table 1. Summary of cistrome, epigenome, and transcriptome data sets included in the nuclear receptor Cistrome web interface

Data set	Species	Factor number	Factor	Data set number
Nuclear receptor	Human	10	AR, ESR1, ESR2, HNF4A, NR3C1, PGR, RARA, RARG, RXR, VDR	66
	Mouse	7	ESRRB, HNF4A, NR1H2, NR3C1, PPARG, RAR, RXR	22
Collaborating factor	Human	18	CDX2, CEBP, CTCF, ERG, FoxA1, FoxA2, GABP, GATA3, GATA6, PML, PolII, RAD21, SRC-3, STAG1, TRIM24, c-Fos, c-Jun, c-MYC	82
	Mouse	6	CEBP, FoxA2, Oct2, PDX1, PU1, PolII	39
Epigenome	Human	12	Ace_H3, H3K14ac, H3K27me3, H3K36me3, H3K4me1, H3K4me2, H3K4me3, H3K9K14ac, H3K9ac, H3K9me3, H3R17me2, Pan-H3	75
	Mouse	3	H3K4me1, H3K4me3, H3K9ac	19
Transcriptome	Human	9	AR, ESR1, ESR2, HNF4A, NR3C1, PGR, RARA, RARG, VDR	35
	Mouse	3	HNF4A, NR1H2, PPARG	5

receptors. These data sets encompass all of the published genome-wide ChIP-chip/seq studies on nuclear receptors and their related factors in humans and mice before 2011, as far as we are aware. We included the ESRRB ChIP-seq conducted in mouse embryonic stem cells but did not include other stem cell ChIP-chip/seq data because of the large number of such data sets that are not necessarily related to the cancer focus of this study. For ChIP-chip data consistency, we did not include any chromosome-wide, custom tiling, or spotted cDNA arrays but did include ChIP-chip on Affymetrix whole genome or promoter tiling arrays because of their stable designs. Model-based analysis of tiling arrays (MAT; ref. 16) and model-based analysis of ChIP-Seq (MACS; ref. 17) were used for ChIP-chip and ChIP-seq peak calling, respectively. In addition, we analyzed 40 gene expression data sets for 11 activation and/or deactivation experiments on nuclear receptors, totaling 319 microarray profiles. A summary of the data analyzed is shown in (Table 1).

Motif analyses

Previous protein structure analysis has suggested that in nuclear receptor dimers, one monomer often binds to DNA much more strongly than the other (10). However, when we applied MDscan for *de novo* motif discovery in the nuclear receptor cistrome sites, the nuclear receptor full-site motifs identified were surprisingly symmetric between the 2 half-sites. In addition, when we collected full-site motif hits in the cistrome sites having sufficiently good overall matches (the summation of the 2 half-site matching scores) to the consensus sequence, the 2 half-sites were also symmetric (Fig. 1A). This suggests that the 2 monomers contribute similarly to the *in vivo* binding, which may differ from *in vitro* binding.

We then examined how the 2 monomers were arranged in directed (DR), everted (ER), or inverted (IR) configurations with variable gaps for different nuclear receptors (see Fig. 1A and Supplementary Figs. S1–S7). Most of the nuclear receptors investigated had only one strong full-site motif, corresponding to their previously known canonical motif. Many other noncanonical motifs, although significantly enriched compared with the genome background, were much weaker than the canonical ones (Fig. 1A), suggesting that the binding sites with noncanonical motifs may be functional in a more context-dependent manner. One interesting exception was ESR1, which had strong enrichment of directed, everted, and inverted motifs.

Some nuclear receptors that form heterodimers with other nuclear receptors can recognize different full-site motifs. For example, RXR recognizes DR5 when dimerizing with RARA in human NB4 cells and DR1 when dimerizing with PPARG in mouse adipocyte cells. Note that RXR and its dimerization partner in adipocytes, PPARG, show noncanonical ER14 and IR3 motifs (Supplementary Figs. S1 and S2) in preadipocytes. For PPARG, the enrichment level of ER14 and IR3 motifs became weaker during adipogenesis and disappeared in mature adipocytes whereas that of DR1 became stronger. For PPARG's dimerization partner RXR, ER14 and IR3 enrichment was also observed in early adipogenesis and DR1 enrichment was observed in mature adipocyte. This suggests that PPARG may have different interaction partners and recognition patterns in early adipogenesis. Further studies are needed to identify these factors and their transcriptional consequences.

Previous studies using *in vitro* gel-shift and protein structure analysis implied that some nuclear receptors could bind half-site motifs and function as monomers *in vivo*. We took all of the nuclear receptor cistrome sites that do not contain
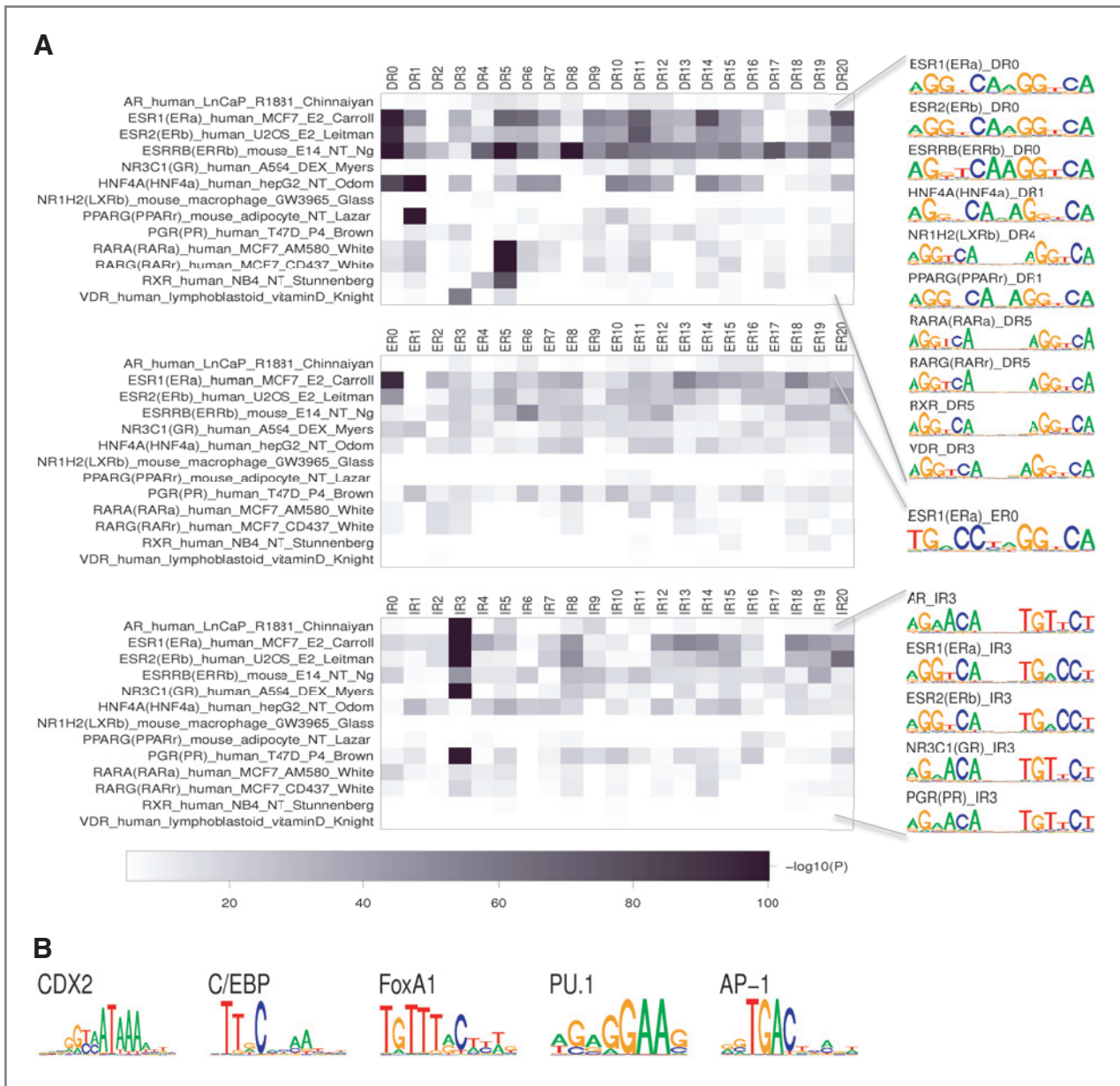
Figure 1. A, enrichment heat map of nuclear receptor full-site motifs arranged in directed (DR), everted (ER), or inverted (IR) patterns spaced by 0 to 20 random nucleotides. One representative data set for each nuclear receptor was selected and is shown in the figure. To the right of the heat map are sequence logos of nuclear receptor full-site motifs retrieved from ChIP-chip/seq peak regions. B, sequence logos of identified nuclear receptor collaborating factors.

a full-site (with DR0-20, ER0-20, and IR0-20 patterns) and searched for half-site occurrences. Using regions 2 kb away from cistrome sites as a random control, we found that RARG had the strongest pattern of half-site enrichment (Supplementary Fig. S8). Other factors showing half-site enrichment include androgen receptor (AR), ESR2, NR3C1, PPARG, and RARA, suggesting that they indeed bind to DNA *in vivo* as a monomer in addition to a dimer (Supplementary Fig. S8). We then examined whether the nuclear receptor peaks with only half-sites were associated (within 50 bp between peak and gene TSS) with significantly more differ-entially expressed genes than random genes. We indeed observed significant association, especially between the half-sites and upregulated genes (Supplementary Fig. S9), which indicates that nuclear receptor binding to half-sites is very likely to be functional. Interestingly, the ESRRB ChIP-seq data from mouse embryonic stem cells showed 3 equally enriched full-site motifs, DR0, DR5, and DR8 (Fig. 1A) but no half-site enrichment (Supplementary Fig. S8). Although ESRRB was previously suggested to bind as a monomer (18), its ChIP-seq data indicate that ESRRB func-tions as a dimmer *in vivo*.

ChIP-chip/seq can pull down targets of transcription factors that interact with the ChIP-ed factor of interest. We therefore conducted a motif analysis to find the most significant collaborating motifs for each nuclear receptor (Fig. 1B and Supplementary Table S2). Among these motifs, there are previously reported and experimentally validated collaborating motifs, including FoxA1 for AR, ESR1, RARA, and RARG; C/EBP for HNF4A, NR3C1, PPARG, and RXR; PU.1 for NR1H2; and CDX2 for HNF4A; there are also newly discovered collaborating motifs, including FoxA1 for PGR; AP-1 for ESR2, NR3C1, and VDR; and PU.1 for RARA and RXR. One interesting phenomenon we noticed is that many of the transcription factors for nuclear receptors, such as FoxA1, C/EBP, PU.1, and CDX2, have relatively short and AT-rich motifs. These motifs are likely the cell type–specific chromatin remodelers that can more easily bind to nucleosome-free regions. Once these pioneering factors pry open the chromatin, nuclear receptors can bind to the DNA and,

with their relatively longer motif patterns, convey specific transcriptional effects.

Binding site distributions

When transcription factor cistromes were first published (19), a surprising finding was that despite the significant promoter enrichment observed, most binding sites were located in introns and distal intergenic regions far away from transcription start sites. With the cistromes of many nuclear receptors at hand, we investigated these findings in a more comprehensive way. For most of the nuclear receptors, the median distance between a binding site and its nearest gene was more than 10 kb far. Stronger binding sites were no closer to the genes, although binding sites were much closer to genes than random genomic regions (Fig. 2A). However, binding sites were often significantly closer to genes that are differentially expressed upon nuclear receptor activation (Fig. 2B). Interestingly, although factors AR, ESR2, HNF4A, NR3C1, PGR, VDR, and
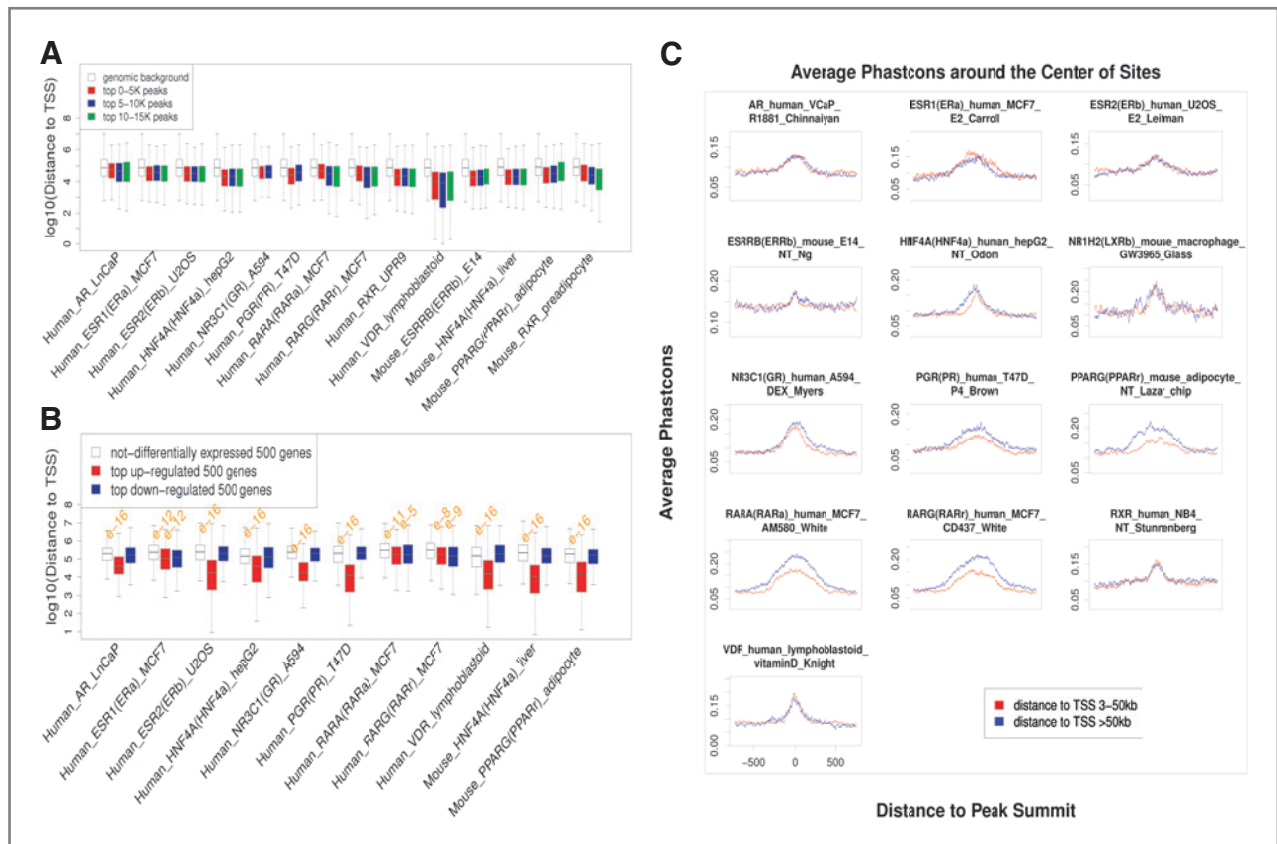
Figure 2. A, top 0–5 K/5–10 K/10–15 K peaks (ranked by P values from small to large) were compared by their distances to the nearest genes, and all the nuclear receptors with at least one data set of more than 10 K peaks are included. No significant differences in peak distance were observed among the 3 groups. B, two groups of genes (upregulated and downregulated; 500 genes) were compared with one group (nondifferentially expressed; 500 genes) by their distances to the nearest peaks, and all the nuclear receptors with at least one ChIP-chip/seq data set coupled with de/activation experimental data set were included. Wilcoxon rank-sum test was used to test significance of distance disparity; significantly small P values are marked above the corresponding boxplot. For all the nuclear receptors, upregulated genes were closer to binding sites than nondifferentially expressed genes; however, similar phenomena were observed in downregulated genes only for ESR1, RARA, and RARG. C, average phastCons conservation score profiles around the 1,200 bp summits of nuclear receptor–binding sites. Two groups of binding sites, with different distances to their nearest genes, were compared by their phastCons conservation score profiles, and no significant variations were observed.
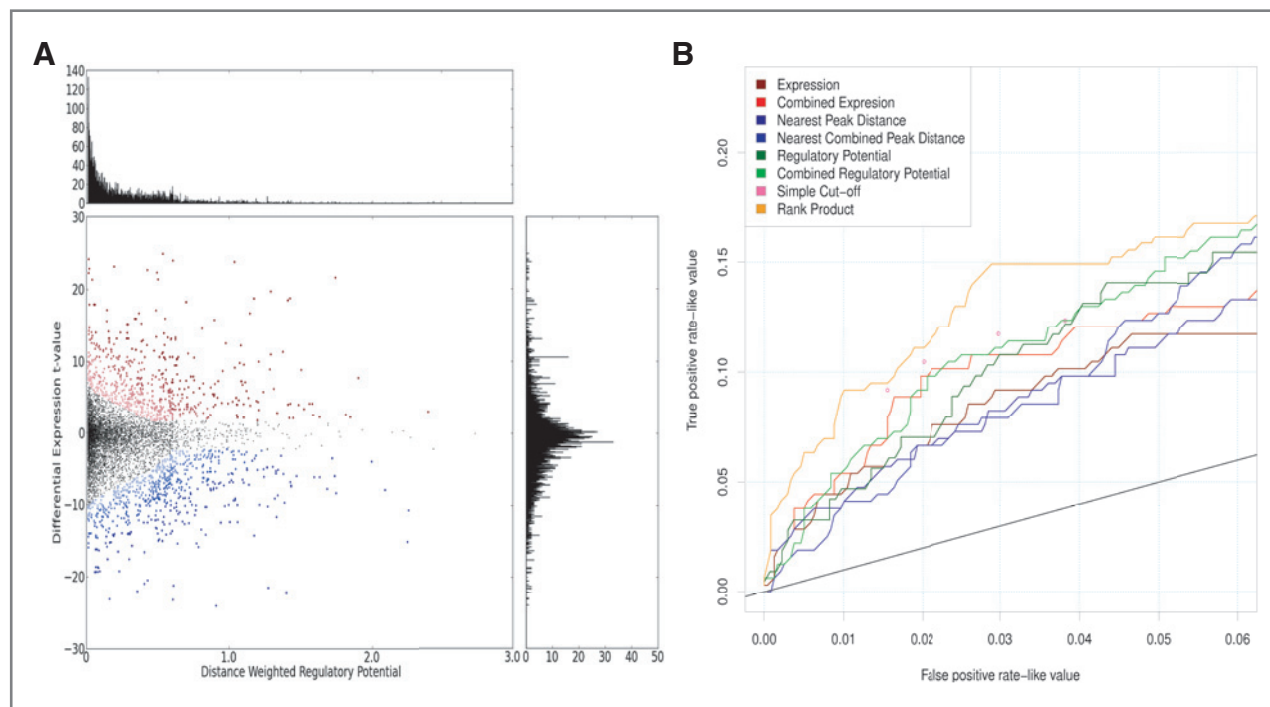
Figure 3. A, scatter plot of genes represented by 2 parameters: the regulatory potential calculated from Brown laboratory's ESR ChIP-chip data set and the differential expression t value calculated from Brown laboratory's expression data set of 12-hour estrogen treatment. Rank product method was used to integrate the 2 parameters and render a rank order list of genes according to their likelihoods of being ESR targets. Red dots represent the top 800 genes that are most likely to be upregulated ESR targets; red dots with darker colors are more likely to be targets than those with lighter colors. Similarly, blue dots represent the top 800 genes that are most likely to be downregulated ESR targets; blue dots with darker colors are more likely to be targets than those with lighter colors. The horizontal histogram represents the distribution of regulatory potential, and the vertical histogram represents the distribution differential expression values. B, receiver operating characteristic–like curve for ESR1 as a validation of our integrated target prediction method. We calculated the correlation values of all the other genes with ESR1 using van de Vijver's breast tumor expression data and defined genes with expression correlations larger than 0.3 as true positives and those with correlations between −0.2 and 0.2 as true negatives. *ESR1* target genes predicted by different approaches were compared.

PPARG were only closer to upregulated genes, *ESR1*, *RARA*, and *RARG* in MCF7 were closer to both up- and down-regulated genes (Fig. 2B). This finding suggests that ESR1, RARA, and RARG have dual functions as transcriptional activators and repressors, whereas other nuclear receptors mainly function as activators.

We investigated the evolutionary conservation of nuclear receptor cistromes in more than 46 vertebrate species. Previous studies from our group and others have reported that the majority of binding sites are not conserved at the sequence level (1). Indeed, the average phastCons conservation score at the 200-bp binding summits was only approximately 0.15. We then divided binding sites into 2 categories on the basis of their distance from a TSS. Interestingly, binding sites closer to genes were not more conserved than those farther away (Fig. 2C and Supplementary Fig. S10). In addition, binding sites near upregulated genes were not more conserved than those near random genes, and binding sites closer to upregulated genes were not always more conserved than those farther away from upregulated genes (Supplementary Fig. S11).

Target gene prediction

One of the most important goals of transcription factor ChIP-chip/seq studies is the identification of direct target genes of the factor. However, as most binding sites land in distal intergenic regions or introns, target gene prediction is not straightforward. Prior studies have often used cutoff values such as differential expression false discovery rate less than 0.05 and at least one binding within 10 kb from the gene TSS to identify targets. However, such cutoff values are arbitrary and ignore the fact that some target genes are more strongly regulated by one factor than others. Techniques, such as Hi-C and ChIA-PET, have been developed to study the genome-wide chromatin interactions but do not have the sensitivity or resolution to link each binding site to its regulated genes. However, these studies found that the general trend of chromatin interactions diminishes in a predictable way with increasing genomic distance. In addition, our preliminary analysis found that enhancer regulation potential is proportional to the number of binding sites near a gene, and this finding suggests that transcription factor binding and regulatory gene target follows a many-to-many relationship. Therefore, by combining differential gene expression profiles with transcription factor cistromes, we should be able to make improved probabilistic prediction of direct target genes of a factor.

Through meta-analysis of different omic data of the same cancer cell line model from multiple studies, we generated consensus cistrome and expression profiles: we combined

multiple ChIP-chip/seq data sets for the same nuclear receptors in the same cell line model to create a consensus peak list, and we combined multiple expression data sets in the same cell line model and condition to give each gene a consensus differential expression *z*-score (see Materials and Methods). We further made probabilistic predictions of the nuclear receptor target genes by integrating cistrome and transcriptome data (see Materials and Methods).

As a validation of our integrated target prediction method that was applied to identify *ESR1* gene targets in MCF7, we calculated the correlation of all the other genes with ESR1 using van de Vijver's breast tumor expression data (20). By defining genes with expression correlations larger than 0.3 as true positives and those with correlations between −0.2 and 0.2 as true negatives, we generated a receiver operating characteristic–like curve of our predictions. Combining multiple expression or ChIP data gave better results than using single expression or ChIP data, and integrating expression with ChIP gave better results than each data type alone and also better results than the simple cutoff method (Fig. 3B).

Discussion

ChIP-chip/seq methods have been increasingly adopted as a powerful approach to study transcription factor regulation in normal physiology and disease. Nuclear receptors are important gene regulators in many cancer systems. We systematically collected publicly available cistrome data for nuclear receptors in cancer cells, for their collaborating transcription factors, and for histone modifications. We also integrated the cistrome data with related differential gene expression data to identify the direct targets of different

nuclear receptors in these cancers. Together, these integrated data not only create a useful resource for the nuclear receptor and cancer community but also provide a more comprehensive view of the genome-wide binding characteristics and regulatory mechanisms of nuclear receptors involved in cancer.

As more related cistrome and transcriptome data become available, we will add them to the current database, such as the NR1D1 ChIP-seq data set published in 2011 (21).

We will refine the regulatory modules, including the collaborating transcription factors and gene targets, of different nuclear receptors in cancers. We are also working on a comprehensive data analysis pipeline (22), so researchers can reuse the public data in combination with their own genomic and epigenomic data to better understand gene regulation in cancers.

References

1. Carroll JS, Meyer CA, Song J, Li W, Geistlinger TR, Eeckhoute J, et al. Genome-wide analysis of estrogen receptor binding sites. Nat Genet 2006;38:1289–97.
2. Fu XD, Goglia L, Sanchez AM, Flamini M, Giretti MS, Tosi V, et al. Progesterone receptor enhances breast cancer cell motility and invasion via extranuclear activation of focal adhesion kinase. Endocr Relat Cancer 2010;17:431–43.
3. Wang Q, Li W, Zhang Y, Yuan X, Xu K, Yu J, et al. Androgen receptor regulates a distinct transcription program in androgen-independent prostate cancer. Cell 2009;138:245–56.
4. Yu J, Mani RS, Cao Q, Brenner CJ, Cao X, Wang X, et al. An integrated network of androgen receptor, polycomb, and TMPRSS2-ERG gene fusions in prostate cancer progression. Cancer Cell 2010;17:443–54.
5. Hua S, Kittler R, White KP. Genomic antagonism between retinoic acid and estrogen signaling in breast cancer. Cell 2009;137:1259–71.
6. Martens JH, Brinkman AB, Simmer F, Francoijs KJ, Nebbioso A, Ferrara F, et al. PML-RARalpha/RXR alters the epigenetic landscape in acute promyelocytic leukemia. Cancer Cell 2010;17:173–85.
7. Iliopoulos D, Jaeger SA, Hirsch HA, Bulyk ML, Struhl K. STAT3 activation of miR-21 and miR-181b-1 via PTEN and CYLD are part of the epigenetic switch linking inflammation to cancer. Mol Cell 2010;39:493–506.
8. Hirsch HA, Iliopoulos D, Joshi A, Zhang Y, Jaeger SA, Bulyk M, et al. A transcriptional signature and common gene networks link cancer with lipid metabolism and diverse human diseases. Cancer Cell 2010;17:348–61.
9. Glass CK, Saijo K. Nuclear receptor transrepression pathways that regulate inflammation in macrophages and T cells. Nat Rev Immunol 2010;10:365–76.
10. Kumar R, Thompson EB. The structure of the nuclear hormone receptors. Steroids 1999;64:310–9.
11. Nuclear Receptor Cancer Cistromes [cited 2011 Jun 10]. Available from: http://cistrome.dfci.harvard.edu/NR_Cistrome.
12. Ochsner SA, Steffen DL, Hilsenbeck SG, Chen ES, Watkins C, McKenna NJ. GEMS (Gene Expression MetaSignatures), a Web resource for querying meta-analysis of expression microarray datasets: 17beta-estradiol in MCF-7 cells. Cancer Res 2009;69:23–6.
13. Chen Y, Meyer CA, Liu T, Li W, Liu JS, Liu XS. MM-ChIP enables integrative analysis of cross-platform and between-laboratory ChIP-chip or ChIP-seq data. Genome Biol 2011;12:R11.
14. Breitling R, Armengaud P, Amtmann A, Herzyk P. Rank products: a simple, yet powerful, new method to detect differentially regulated genes in replicated microarray experiments. FEBS Lett 2004;573:83–92.
15. Klisch TJ, Xi Y, Flora A, Wang L, Li W, Zoghbi HY. *In vivo* Atoh1 targetome reveals how a proneural transcription factor regulates cerebellar development. Proc Natl Acad Sci U S A 2011;108:3288–93.
16. Johnson WE, Li W, Meyer CA, Gottardo R, Carroll JS, Brown M. Model-based analysis of tiling-arrays for ChIP-chip. Proc Natl Acad Sci U S A 2006;103:12457–62.

17. Zhang Y, Liu T, Meyer CA, Eeckhoute J, Johnson DS, Bernstein BE. Model-based analysis of ChIP-Seq (MACS). Genome Biol 2008;9: R137.

18. Gearhart MD, Holmbeck SM, Evans RM, Dyson HJ, Wright PE. Monomeric complex of human orphan estrogen related receptor-2 with DNA: a pseudo-dimer interface mediates extended half-site recognition. J Mol Biol 2003;327:819–32.

19. Carroll JS, Liu XS, Brodsky AS, Li W, Meyer CA, Szary AJ, et al. Chromosome-wide mapping of estrogen receptor binding reveals long-range regulation requiring the forkhead protein FoxA1. Cell 2005;122:33–43.

20. van de Vijver MJ, He YD, van't Veer LJ, Dai H, Hart AA, Voskuil DW, et al. A gene-expression signature as a predictor of survival in breast cancer. N Engl J Med 2002;347:1999–2009.

21. Feng D, Liu T, Sun Z, Bugge A, Mullican SE, Alenghat T. A circadian rhythm orchestrated by histone deacetylase 3 controls hepatic lipid metabolism. Science 2011;331:1315–9.

22. Cistrome [cited 2010 Oct 20]. Available from: http://cistrome.org/ap/.